

7. Blade motion and rotor control

2020

Prof. SangJoon Shin



Overview

- ❖ I. Equilibrium of hinged blades
- ❖ II. Control of the hinged rotor in hover
- ❖ III. Blade flapping motion
- ❖ IV. Rotor control in forward flight
- ❖ V. Blade motion in the plane of the disk

Introduction

- ❖ Rotor moving edgewise in the air : forward flight
 - two standard means available to overcome dissymmetry of lift
 1. Hinged at the roots so that no moments can be transmitted
 - Control can be achieved by tilting the hub axis until the resultant rotor vector points in the desired direction
 2. Rigidly attached to the shaft but cyclically feathered
 - Decrease pitch on advancing side / increasing pitch on retreating side
 - Equalize the lift around the disk

I. Equilibrium of hinged blades

- ❖ Normal flapping blade... effectively mounted to the hub on a universal joint – free to flap, lead, or lag, but always fixed in pitch

1. Equilibrium about the flapping hinge

- Forces acting on the blade in flapping direction
 - lift, centrifugal forces, weight(negligible)
- Elemental centrifugal forces (Fig. 7-3)

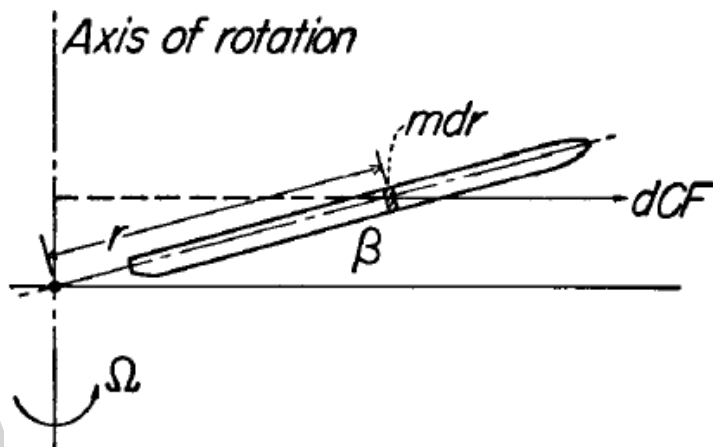


Fig. 7-3 Centrifugal force distribution

$$d(C.F.) = (mdr)\Omega^2 r \cos \beta \quad (1)$$

m : mass per unit length
 Ω : rotational speed
 r : radius of the element
 β : blade flapping angle

I. Equilibrium of hinged blades

- Component of centrifugal force perpendicular to the blade

$$d(C.F.) \sin \beta = mdr\Omega^2 r\beta \quad (2)$$

→ varies linearly with the radius →

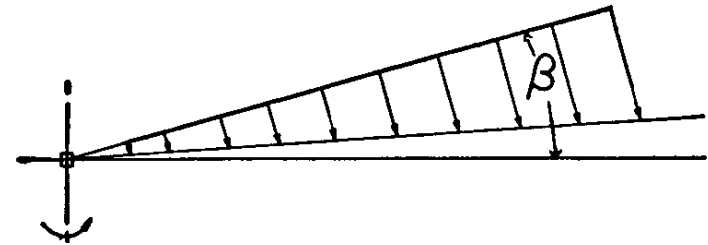


Fig. 7-4 Centrifugal force distribution perpendicular to blade.

- Moment exerted by C.F. about the flapping hinge

$$C.F. \text{ Moment} = \frac{1}{3}R(M\Omega^2 R\beta) = \frac{2}{3}(CF)R\beta \quad (3)$$

- Lift force distribution * $M = mR$, the blade mass

Untwisted constant-chord blade	Ideally twisted constant-chord
inflow varies linearly with radius	inflow is constant along the radius

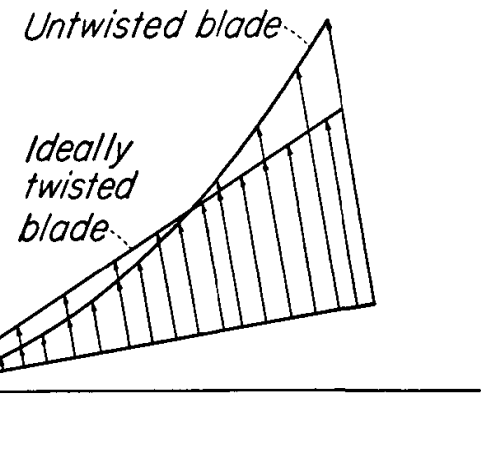


Fig. 7-5 Lift distributions along blade.

I. Equilibrium of hinged blades

- Elemental lift
$$\frac{dL}{dr} = c_l \frac{\rho}{2} \Omega^2 r^2 c \quad (4)$$

- For an ideally twisted constant-chord blade

$$c_l = \alpha_r \alpha = \alpha \left(\theta_t \frac{R}{r} - \frac{v}{\Omega r} \right) \quad (4a)$$

$$\rightarrow \text{Lift} = \text{constant} \times r$$

- Lift of an ideally twisted blade varies with radius
- For an untwisted blade, α_r roughly constant, lift varies $\propto r^2$

$$\text{Lift moment} \left\{ \begin{array}{l} \frac{2}{3} R \times \text{lift} \text{ (for ideal twist)} \end{array} \right. \quad (5)$$

$$\left\{ \begin{array}{l} \frac{4}{3} R \times \text{lift} \text{ (no twist and no taper)} \end{array} \right. \quad (6)$$

I. Equilibrium of hinged blades

- Coning angle β

- $\beta = \frac{\text{blade lift}}{C.F.}$ (for ideally twisted) (7)

- $\beta = \frac{\frac{9}{8} \text{blade lift}}{C.F.}$ (untwisted, constant-chord) (8)

→ β in hovering $\sim C_T$

2. Equilibrium about the drag hinge

- ❖ component of C.F. perpendicular to the blade toward zero lag (Fig. 7-6)

$$d(C.F.) = m\Omega^2 r dr (\zeta - i)$$

* ζ = lag angle

* i = angle between no lag position and line of action of C.F.

- From Fig. 7-6, $ir = \zeta(r - e)$
 $i = \zeta \left(1 - \frac{e}{r}\right)$

$$\therefore d(C.F.) = m\Omega^2 r dr \zeta \left[1 - \left(1 - \frac{e}{r}\right)\right] = m\Omega^2 e \zeta dr \dots \text{constant along the span} \quad (9)$$

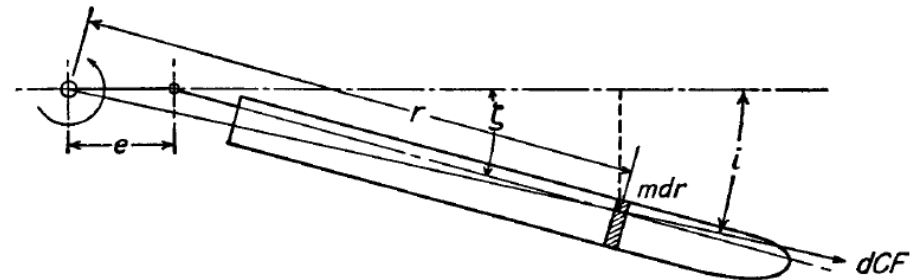


Fig. 7-6 Geometry of blade about lag hinge.

I. Equilibrium of hinged blades

- ❖ Moment of the centrifugal force about the lag hinge

$$C.F. \text{ moment} = mRe\Omega^2 R_{c.g.}\zeta = Me\Omega^2 R_{c.g.}\zeta \quad (10)$$

* $R_{c.g.}$: distance from axis of rotation to the blade c.g.

- ❖ Aerodynamic forces

- Denote resultant force as F , point of application as $R_{d.f.}$

$$\text{Aerodynamic Moment} = FR_{d.f.}$$

- Equating with C.F. moment,

$$FR_{d.f.} = M\Omega^2 R_{c.g.}e\zeta \quad \text{or} \quad F = \frac{M\Omega^2 R_{c.g.}e\zeta}{R_{d.f.}} \quad (11)$$

- Equating the shear forces @ lag hinge (Fig. 7-7)

$$\text{Torque}/e = F \cos \zeta + M\Omega^2 R_{c.g.} \sin \zeta = F + M\Omega^2 R_{c.g.}\zeta \quad (12)$$

I. Equilibrium of hinged blades

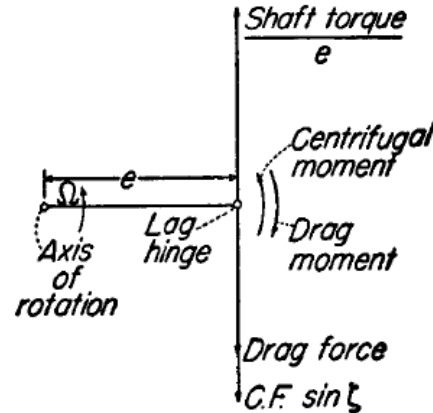


Fig. 7-7 Force and moment equilibrium at lag hinge.

(12) \rightarrow (11)

$$\text{Torque}/e = M\Omega^2 R_{c.g.} \zeta \frac{e}{R_{d.f.}} + M\Omega^2 R_{c.g.} \zeta = \zeta (M\Omega^2 R_{c.g.}) \left(\frac{e}{R_{d.f.}} + 1 \right)$$

$$\zeta = \frac{\text{Torque}}{M\Omega^2 R_{c.g.} e \left(\frac{e}{R_{d.f.}} + 1 \right)} \quad (13)$$

- mean drag angle is a function of $\text{torque}/\Omega^2 \rightarrow C_Q$
- Relatively insensitive to change in $R_{d.f.}$.

II. Control of the hinged rotor in hover

- ❖ Sudden rotation of control axis (Fig. 7-11)
 - Change in pitch angle of the blade
→ Lift increase → Blade moves, or “flaps” → Continues until the plane of the blades is again perpendicular to the control axis @ which position no cyclic-pitch changes occur
 - Some delay between a rapid control angle change and the re-alignment of the rotor disk
→ extremely small
 - Differences when the rotor is moving edgewise through the air (Fig. 7-12)

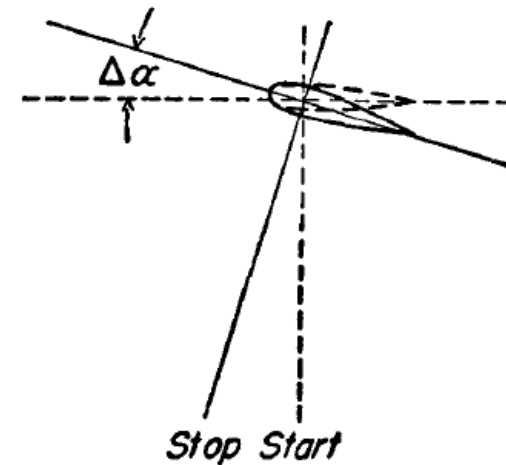


Fig. 7-11 Change in blade angle of attack due to shaft tilt.

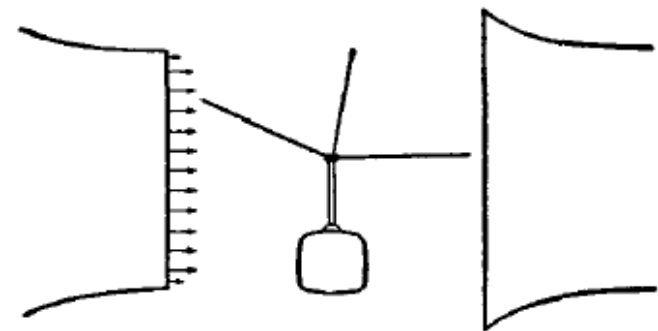


Fig. 7-12 Rotor model in wind tunnel.

III. Blade flapping motion

1. Flapping as represented by a Fourier series

- Flapping motion

$$\beta = a_0 - a_1 \cos \psi - b_1 \sin \psi - a_2 \cos 2\psi - b_2 \sin 2\psi \dots \quad (14)$$

β : angle between the control axis and the blade

ψ : azimuth angle (Fig. 7-13)

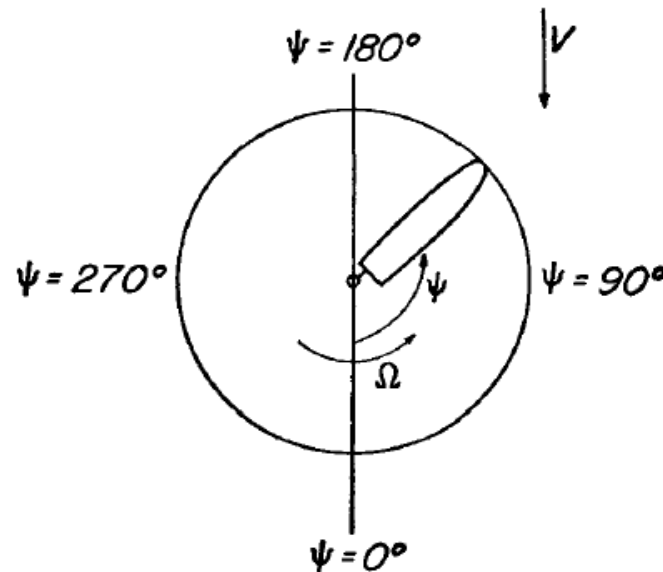


Fig. 7-13 Azimuth angle measurement.

III. Blade flapping motion

2. Geometrical interpretation of the Fourier coefficient

- a_0 : flapping angle independent of the blade azimuth angle ψ in hover
 $\beta = a_0$ (Fig. 7-14 ↓)
- a_1 : amplitude of a pure cosine motion
 $\beta = -a_1 \cos \psi$ (Fig. 7-15, 7-16 →)
- b_1 : amplitude of a pure sine motion
 $\beta = -b_1 \sin \psi$ (Fig. 7-17, 7-18)

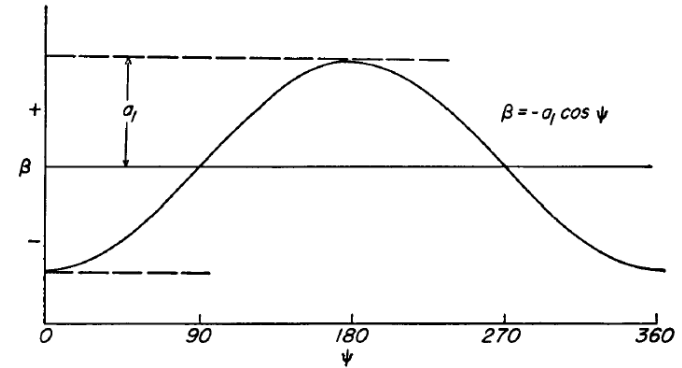


Fig. 7-15 Graphical representation of first harmonic cosine blade motion.

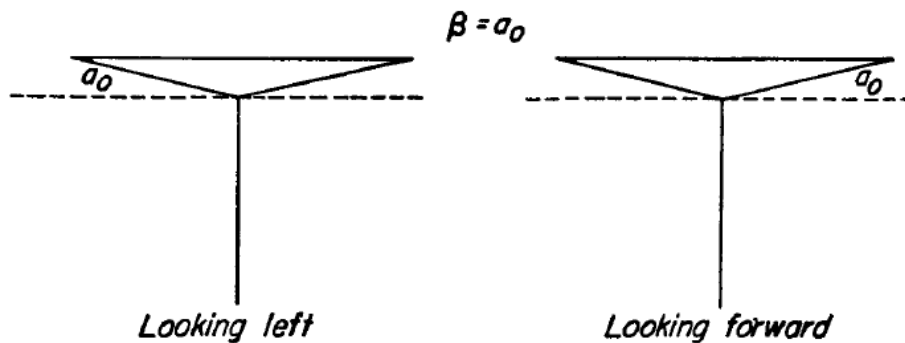


Fig. 7-14 Hovering case wherein $\beta = a_0$.

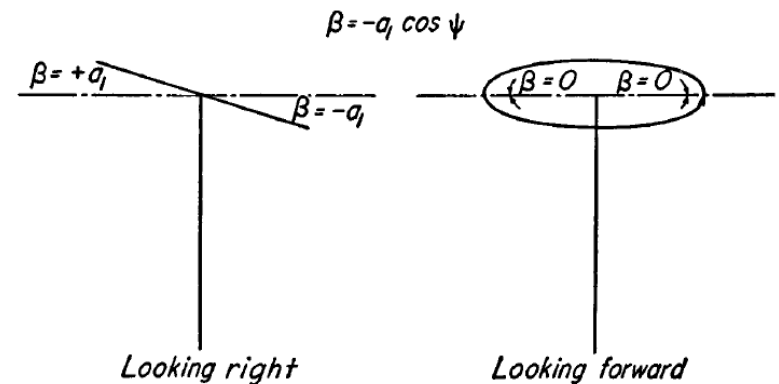


Fig. 7-16 Rotor executing first harmonic cosine blade motion.

III. Blade flapping motion

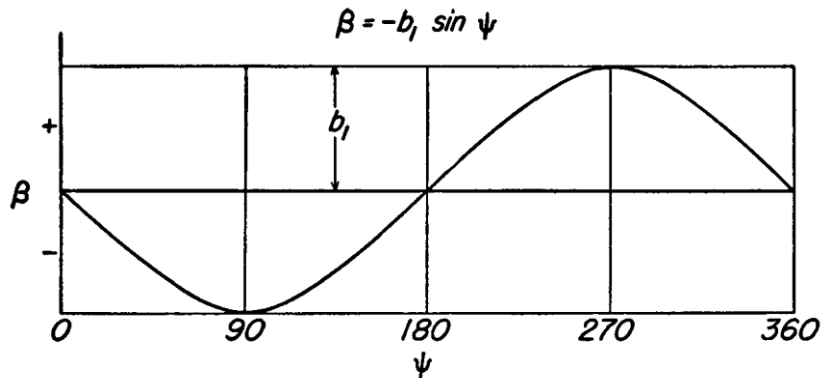


Fig. 7-17 Graphical representation of first harmonic sine blade motion.

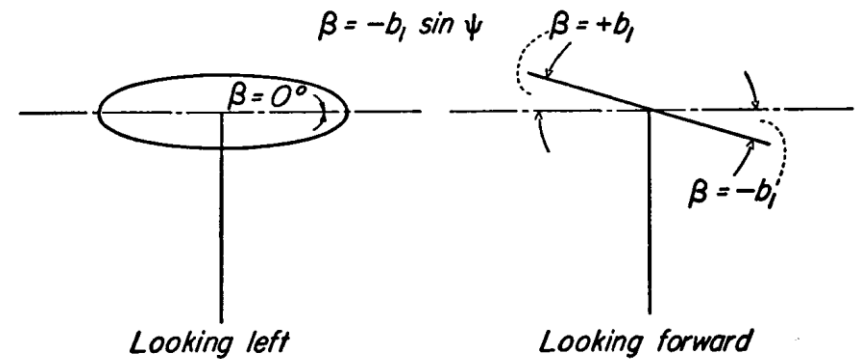


Fig. 7-18 Rotor executing first harmonic sine blade motion.

- (-) sign → result in plus values for the a_1 and b_1 coefficients
in normal forward flight

a_2 : amplitudes of the higher harmonics
 $\beta = -a_2 \cos 2\psi$ (Fig. 7-17, 7-16)

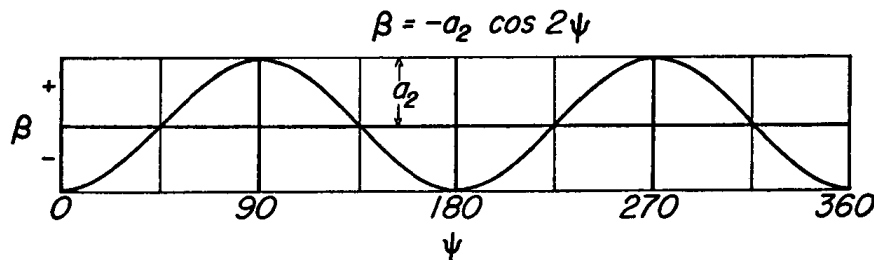


Fig. 7-19 Graphical representation of second harmonic cosine blade motion.

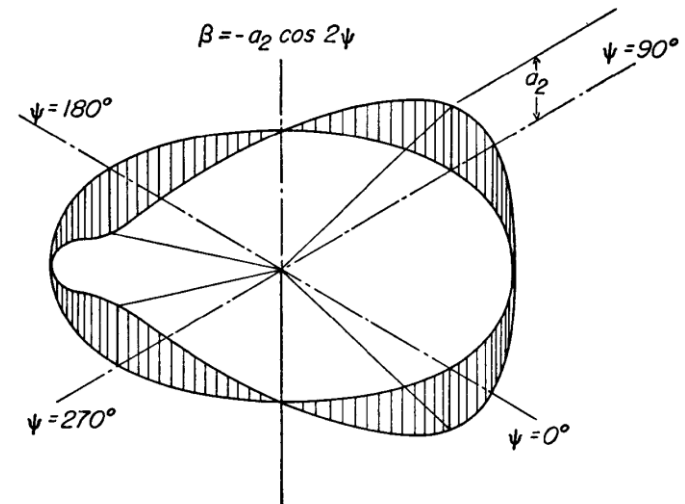


Fig. 7-20 Rotor executing second harmonic cosine blade motion.

III. Blade flapping motion

3. Physical explanation of the existence of the component motions

- ❖ An infinite number of terms in Fourier series exactly describes any arbitrary motion. However, only a few terms are necessary.
- ❖ Magnitude of a typical flapping motion in forward flight

$$a_0 = 8.7^\circ, a_1 = 6.1^\circ, b_1 = 3.9^\circ, a_2 = 0.5^\circ, b_2 = -0.1^\circ$$

- ① Coning angle, a_0 ... depend on the magnitudes of 2 primary moments about the flapping hinge
- Thrust moment (Fig. 7-21)
 - C.F. moment

Hover... large inflow (induced), loading toward tips, larger coning angle (9°)

Min. power... small inflow (small induced), loading more inboard, smaller coning angle (8°)

High speed... large inflow (parasite), loading toward tips, larger coning angle (9°)

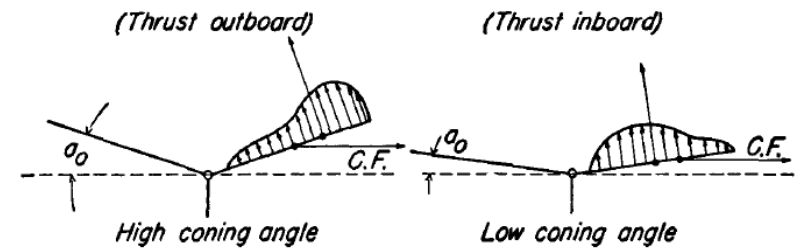


Fig. 7-21 Effect of thrust distribution on coning angle.

III. Blade flapping motion

- ② Backward tilt, $a_1 \dots \psi = 90^\circ \rightarrow$ lift increase \rightarrow flapping up (Fig. 7-23)
 - AoA decrease (Fig. 7-24) no unbalanced force for blade with no inertial forces
 - To consider blade mass and air damping, blade as a dynamic system
- \rightarrow 1 DOF system (Fig. 7-25)

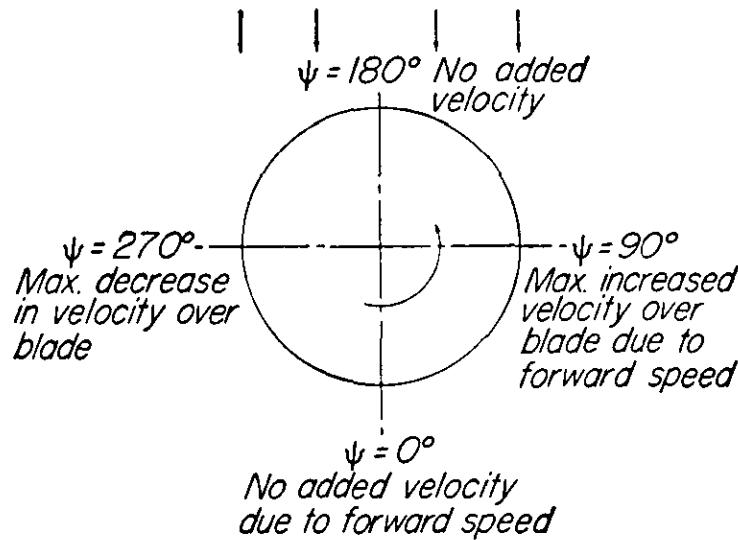


Fig. 7-23 Effect of forward speed on velocity distribution.

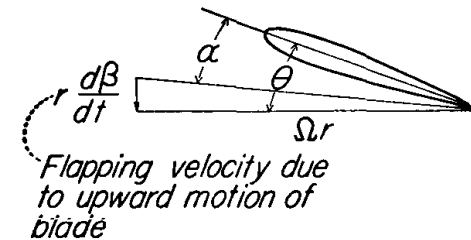


Fig. 7-24 Effect of blade flapping on element angle of attack.

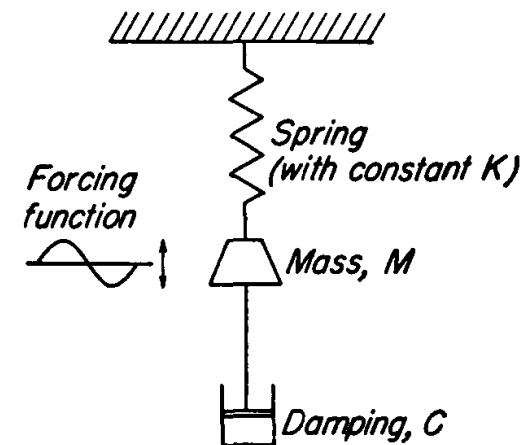


Fig. 7-25 Mechanical analogy to a flapping blade.

III. Blade flapping motion

- Force-displacement phase to the frequency of the forced vibration (Fig. 7-26)

- Φ : phase angle between the max. applied force and max. displacement

- $\frac{c}{c_l}$: ratio of the actual damping to critical damping

- When $\frac{\omega}{\omega_n} = 1 \rightarrow$ phase angle $\phi = 90^\circ$ and is independent of the amount of damping

- Flapping blade (Fig. 7-2)

$$\omega_n = \sqrt{\frac{K}{\tau}} \text{ radians/second} \quad (15)$$

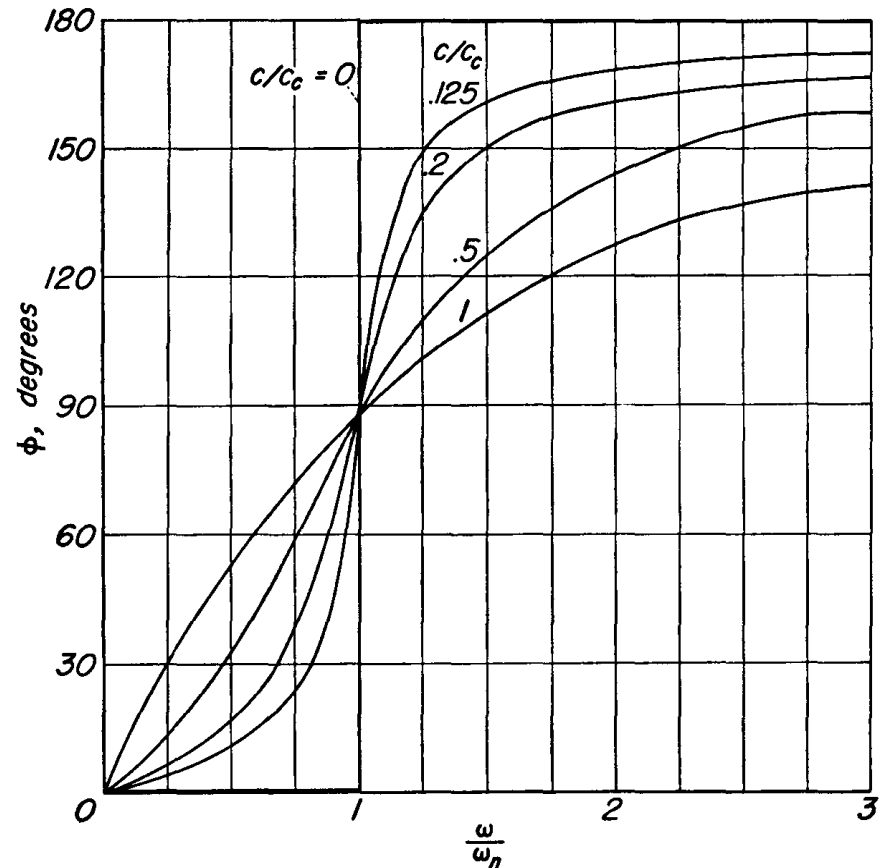


Fig. 7-26 Relation between force-displacement phase and frequency for system with various amounts of damping.

III. Blade flapping motion

- Simple flapping rotor with flapping hinge on the axis of rotation

$$C.F. \text{ moment} = \int_0^R \Omega^2 r^2 \beta m dr = M \Omega^2 \beta \frac{R^2}{3} \quad (17)$$

$$\text{Restoring moment} = K \beta \quad (K = M \Omega^2 \frac{R^2}{3}) \quad (18)$$

$$I = \frac{1}{3} M R^2, \quad \omega_n = \sqrt{\frac{K}{I}} = \sqrt{\Omega^2} = \Omega \quad (19)$$

- When hinge offset = h,

$$\omega_n = \Omega \sqrt{1 + \frac{3h}{2R}}$$

- Exciting air forces... 1/rev $\rightarrow \frac{\omega}{\omega_n} = 1$

\rightarrow force – displacement phase = 90°

- Maximum flapping at $\psi = 180^\circ$

Minimum flapping at $\psi = 0^\circ$

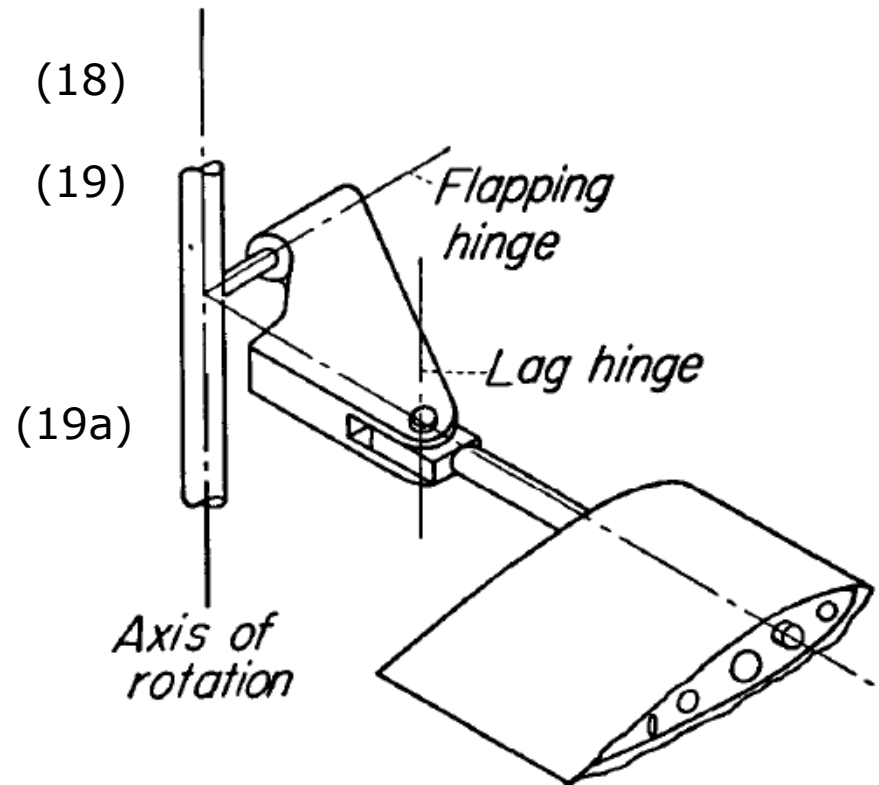


Fig. 7-2 Flapping blade

III. Blade flapping motion

- ③ Sideward tilt, b_1 , ... may be viewed as arising from coning, a_0
- Coned rotor (Fig. 7-27a) : Difference in AoA between front and rear of the blades due to forward speed
 - No coning (Fig. 7-27b) : effect of forward velocity is identical

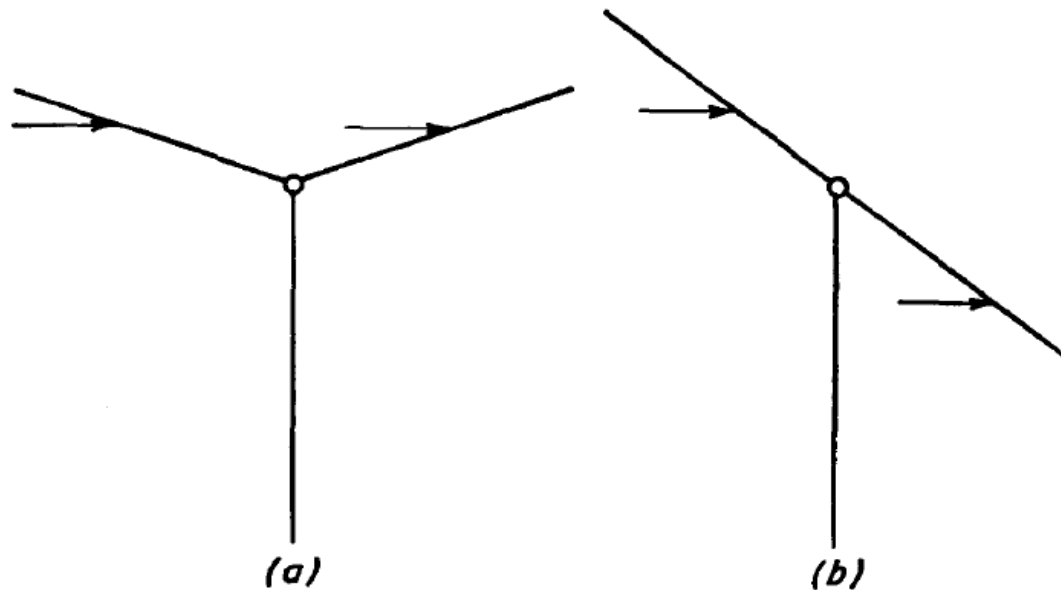


Fig. 7-27 (a) With coning
(b) Without coning

III. Blade flapping motion

- Fig. 7-28 : force is maximum at $\psi = 180^\circ$, minimum at $\psi = 0^\circ$.
 - Force-displacement phase of 90°
 - Max. flapping at $\psi = 270^\circ$, min. at $\psi = 90^\circ$
 - $a + b_1$ motion because of coning. b_1 ... same order as a or larger
- b_1 tilt is very sensitive to variation in inflow
 - assumed as uniform for forward flight performance analysis
 - However, for low forward speed, $v \sim$ quite large at the rear → b_1 increase
- At higher forward flight speed, inflow decreases, and becomes uniform

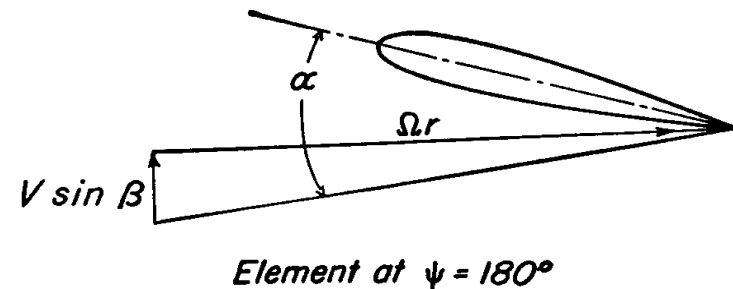
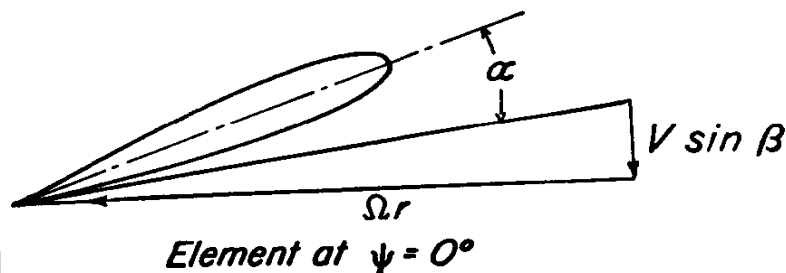


Fig. 7-28 Effect of rotor coning on blade section angles of attack.

III. Blade flapping motion

④ Higher harmonics

- $a_2, b_2, a_3, b_3 \dots$ weaving of the blade in and out of the surface of the core
- Presence of the forces which produce higher harmonic motions
- Asymmetric flow pattern, reverse flow region *Flapping velocity* $\propto \sin^2 \psi$
- Little importance on control and performance, but extremely important for vibration and stresses

⑤ Effect of blade mass on flapping motion

- $a_0 \dots$ directly affected by blade mass
- $a_1 \dots$ independent of blade mass since exciting forces act on resonant system
- $b_1 \dots$ in resonance \rightarrow independent of blade mass
but exciting forces proportional to a_0 , which is proportional to blade mass
- Blade mass increases to infinity $\rightarrow b_1$ decreases to zero
- Higher harmonics... forced vibration well above resonance, goes to zero when blade mass \uparrow

IV. Rotor control in forward flight

- ❖ Tip-Path Plane (TPP) tilts backwards and sideways (by a_1 and b_1) w.r.t. control axis / resultant thrust perpendicular to TPP
→ govern the control of helicopter
- ❖ Hover... TPP exactly perpendicular to control axis
 - Forward Flight... similar, but not exactly perpendicular (Fig. 7-29)
 - TPP tilts faster than the control axis tilts (both for forward and rearward
→ instability of the rotor w.r.t. AoA -> control is more sensitive as forward speed increases

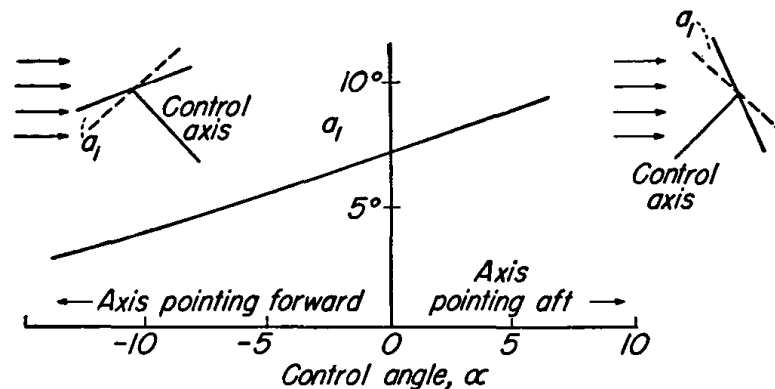


Fig. 7-29 Variation of longitudinal tip-path plane tilt with control axis tilt.

IV. Rotor control in forward flight

- ❖ How to achieve the desired control axis tilt
 - Physically tilting the rotor shaft ("direct control") ... autogyro
 - Mechanically awkward in helicopters → 2 methods to solve

- ① Rotor hub tilting (Fig. 7-30)
 - Separation of the shaft axis and control (hub) axis
 - The hub axis then becomes the control axis
- ② Means for cyclically varying blade pitch (Fig. 7-31)
 - Pitch will be always constant w.r.t. the plane of swash plate

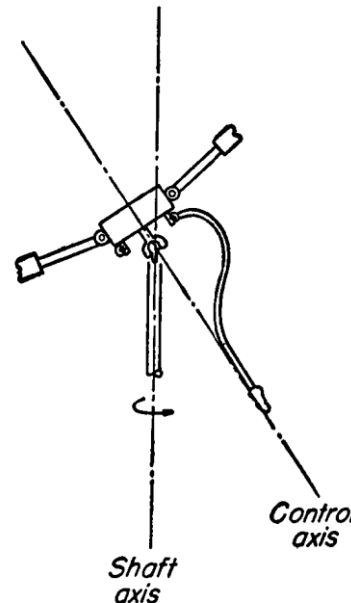


Fig. 7-30 Control by tilting hub with respect to shaft.

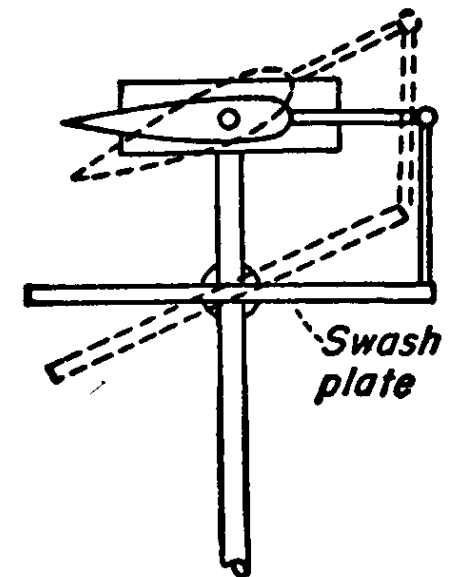


Fig. 7-31 Control by cyclic pitch.

IV. Rotor control in forward flight

❖ Basic equalities of flapping and feathering

- Fig. 7-32... Control axis vertical, TPP tilts rearward by an amount a_1
 - Low pitch on the advancing side, high on the retreating side
- Fig. 7-33... Blade feathering w.r.t. TPP = blade flapping w.r.t. control axis
- Fore and aft (a_1) flapping w.r.t. control axis
 - lateral (β_1) feathering w.r.t. TPP

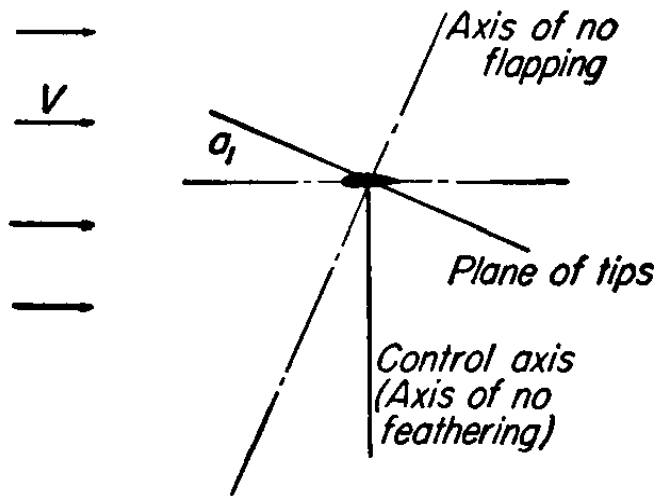
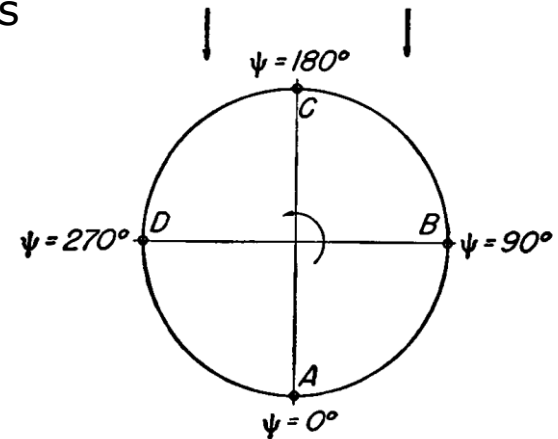


Fig. 7-32 Flapping rotor in forward flight.



With respect to control axis

A = Flapping full down
 B = Flapping zero
 C = Flapping full up
 D = Flapping zero

With respect to tip-path plane

Feathering zero
 Feathering max. down
 Feathering zero
 Feathering max. up

Fig. 7-33 Blade positions with respect to control axis and tip-path plane.

IV. Rotor control in forward flight

❖ Geometrical relationships among

→ Fig. 7-34

Axis of no feathering (control axis)

Axis of no flapping (TPP)

Intermediate shaft axis

- Flapping motion w.r.t. control axis

$$\beta = a_0 - a_1 \cos \psi - b_1 \sin \psi - a_2 \cos 2\psi - b_2 \sin 2\psi \quad (20)$$

- Feathering motion w.r.t. TPP

$$\theta = A_0 - A_1 \cos \psi - B_1 \sin \psi - A_2 \cos 2\psi - B_2 \sin 2\psi$$

- Subscripts... w.r.t. shaft axis

$$\alpha = \alpha_s - B_{1s} \quad (21)$$

$$A_0 = A_{0s} \quad (22)$$

$$a_0 = a_{0s} \quad (23)$$

$$a_1 = a_{1s} + B_{1s} \quad (24)$$

$$b_1 = b_{1s} - A_{1s} \quad (25)$$

$$a_2 = a_{2s} \quad (26)$$

$$b_2 = b_{2s} \quad (27)$$

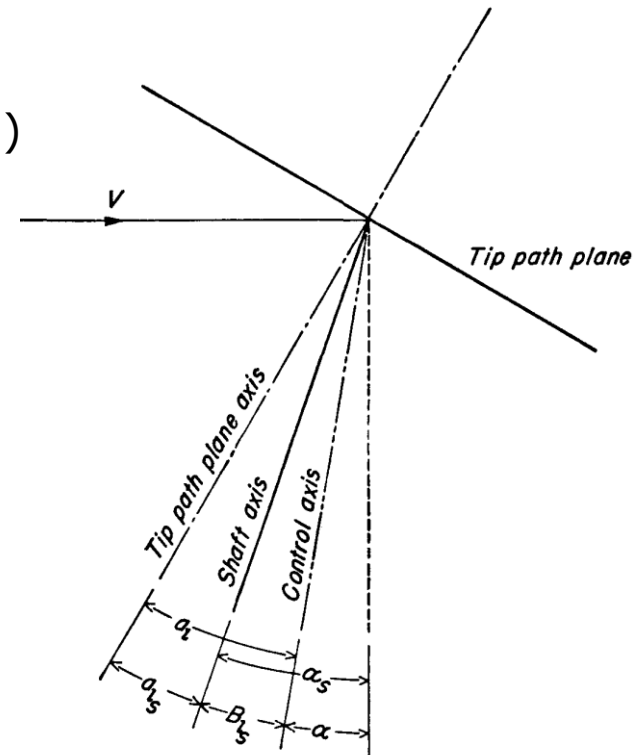


Fig. 7-34 Flapping—feathering relationships.

* a : Aoa of the perpendicular to the control axis with the relative wind

IV. Rotor control in forward flight

- ❖ Fixed resultant force vector in space for a given weight, parasite drag, speed (Fig. 7-35) → TPP fixed → flapping motion completely determined → control axis determined
- Orientation determined : resultant force vector / TPP / control axis
- ❖ 3 possible shaft angles and feathering controls for identical flight conditions (Fig. 7-36)
- Fuselage attitude and control position may vary due to different CG position → no effect on the rotor control in space, except secondary influence

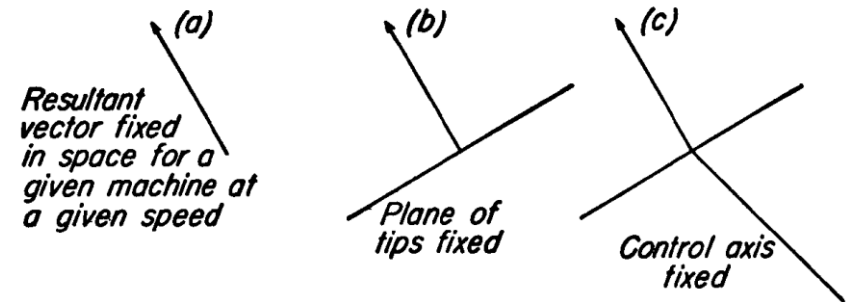


Fig. 7-35 Quantities that are fixed in space for a helicopter in a given flight condition.

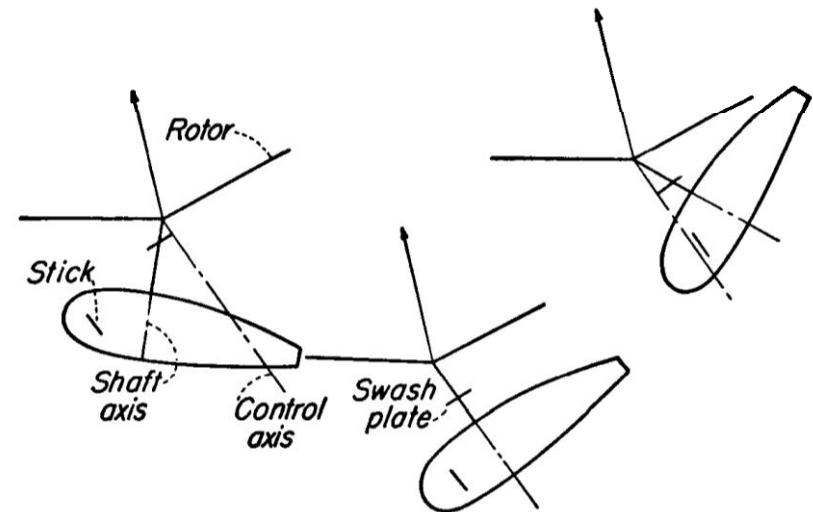


Fig. 7-36 Helicopter in a given flight condition with different combinations of shaft angle and feathering control.

V. Blade motion in the plane of the disk

1. Sources of in-plane blade motion...

- ❖ Periodic blade motion arises from 2 sources
 - ① periodically varying aerodynamic forces... variation in velocity and AoA
 - ② periodically varying mass forces... TPP tilt
 - Fig. 7-37 TPP tilt in hover, control axis still vertical
 - Blade flapping by a_{1s} → CG of the forward blade nearer to the axis of rotation (shaft axis) → to maintain the angular momentum, forward blade must move faster, rearward blade slower → blades move back and forth as they rotate

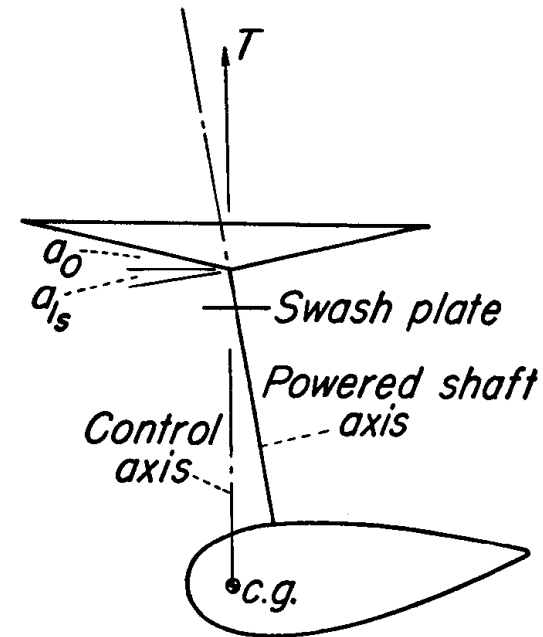


Fig. 7-37 Hovering helicopter illustrating the source of in-plane blade motion.

V. Blade motion in the plane of the disk

❖ Two different axis systems and the resulting forces / motion

- Motion w.r.t. shaft axis... flapping motion

$$\beta_s = a_0 - a_{1s} \cos \psi \quad (28)$$

→ Two periodic torques about the shaft axis

- a. Due to lift acting in the plane perpendicular to the shaft

$$\text{Lift torque component perpendicular to shaft} = T_b r_{a.f.} a_{1s} \sin \psi \quad (29)$$

T_b : thrust per blade

$r_{a.f.}$: radius of the resultant lift on blade

a_{1s} : fore and aft flapping w.r.t. shaft

- b. Periodic "mass force" torque due to periodically changing MOI

- Caused by masses moving radially in a rotating plane ("Coriolis force")

V. Blade motion in the plane of the disk

2. Coriolis force

- ❖ Fig. 7-38... Point mass moves radially outward → tangential velocity increase → resists tangential acceleration → exert a force to the right on the rotating plane

- ❖ Tangential acceleration

$$\frac{d(\Omega r)}{dt} = \Omega \frac{dr}{dt} = \Omega V_{\text{radial}}$$

- ❖ Second component ... changing direction of radial velocity vector in space

$$(\text{Vector length}) \times \frac{d\theta}{dt} \rightarrow \Omega V_{\text{radial}}$$

$$\text{Resultant acceleration} = 2\Omega V_{\text{radial}}$$

$$\text{Coriolis force } F_{\text{coriolis}} = 2mV_{\text{radial}}\Omega \quad (30)$$

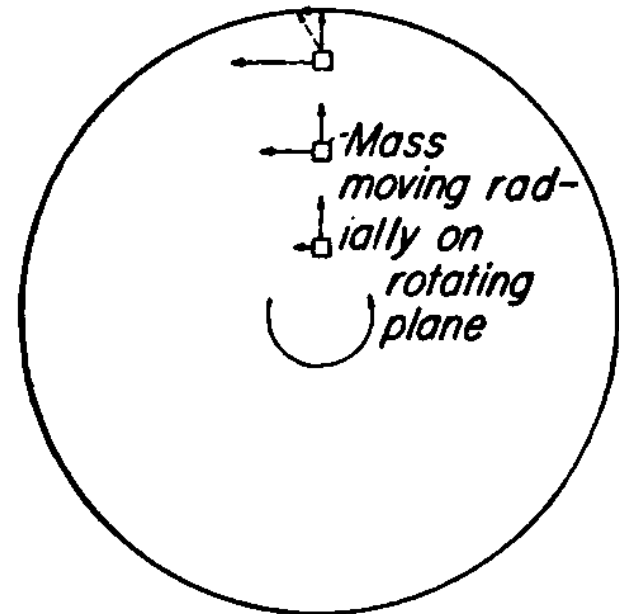


Fig. 7-38 Origin of Coriolis forces.

V. Blade motion in the plane of the disk

- ❖ Coriolis torque acting on Hovering rotor (Fig. 7-37)
 - w.r.t. rotor shaft, a blade element moves outward with a velocity

$$\frac{d(r \cos \beta_s)}{dt} = -r \sin \beta_s \frac{d\beta_s}{dt} = -r \beta_s \dot{\beta}_s \quad (31)$$

$$\beta_s = a_0 - a_{1s} \cos \psi, \quad \dot{\beta}_s = a_{1s} \Omega \sin \psi$$

$$V_{radial} = r \beta_s \dot{\beta}_s = -r \Omega \left(a_0 a_{1s} \sin \psi - \frac{a_{1s}^2}{2} \sin 2\psi \right) \quad (32)$$

* Negligible order

- ❖ Coriolis torque

$$Torque_{Coriolis} = - \int_0^R 2r \Omega^2 a_0 a_{1s} \sin \psi m dr = - \frac{2}{3} MR^2 a_0 a_{1s} \Omega^2 \sin \psi \quad (33)$$

- Uniform blade

$$a_0 = \frac{3r_{a.f.} T_b}{M(\Omega R)^2} \quad (34) \quad \rightarrow \quad Torque_{Coriolis} = -2T_b r_{a.f.} a_{1s} \sin \psi \quad (35)$$

... depends on T_b and a_{1s} , but not on the blade mass

V. Blade motion in the plane of the disk

3. Equation of motion for blade in lag

- Spring restoring torque

$$C.F. torque = \frac{MR}{2} e\Omega^2 \zeta \quad (36)$$

- Equating all torques to the angular acceleration,

$$T_{aero} - T_{Coriolis} - T_{spring} = I\ddot{\zeta} \quad (37)$$

- Substituting,

$$T_b r_{a.f.} a_{1s} \sin \psi - 2T_b r_{a.f.} a_{1s} \sin \psi - Me\Omega^2 \frac{R}{2} \zeta = I\ddot{\zeta} \quad (38)$$

↑
Increase lag angle
for (+) a_1 motion

↑
(+) a_1 motion → MOI
decrease → lead motion → (-)

↙
Always resists the motion

- Rearranging,

$$I\ddot{\zeta} + Me\Omega^2 \frac{R}{2} \zeta = -T_b r_{a.f.} a_{1s} \sin \psi \quad (39)$$

- Damping neglected. Possible sources {
 - aerodynamic damping
 - physical dampers at the blade root

V. Blade motion in the plane of the disk

- Solution of Eqn. (39) ... assuming a solution of form $\zeta = \zeta_0 \sin \omega t$

$$\zeta_0 = \frac{-T_b r_{a.f.} a_{1s}}{\frac{MR}{2} e \Omega^2 - I \omega^2}, \quad \Omega = \omega \quad (41)$$

- For a uniform blade,

$$I = \frac{1}{3} MR^2 \rightarrow \zeta_0 = \frac{\frac{2}{3} a_0 a_{1s}}{\frac{2}{3} - \frac{e}{R}} \quad (42)$$

- For the limiting case of $e \rightarrow 0$,

$$\zeta = a_0 a_{1s} \sin \psi \quad (43)$$

- Fig. 7-39... For a rotor with blades hinged at the center of rotation, Coriolis forces cause the blades to move always at constant velocity w.r.t. TPP.

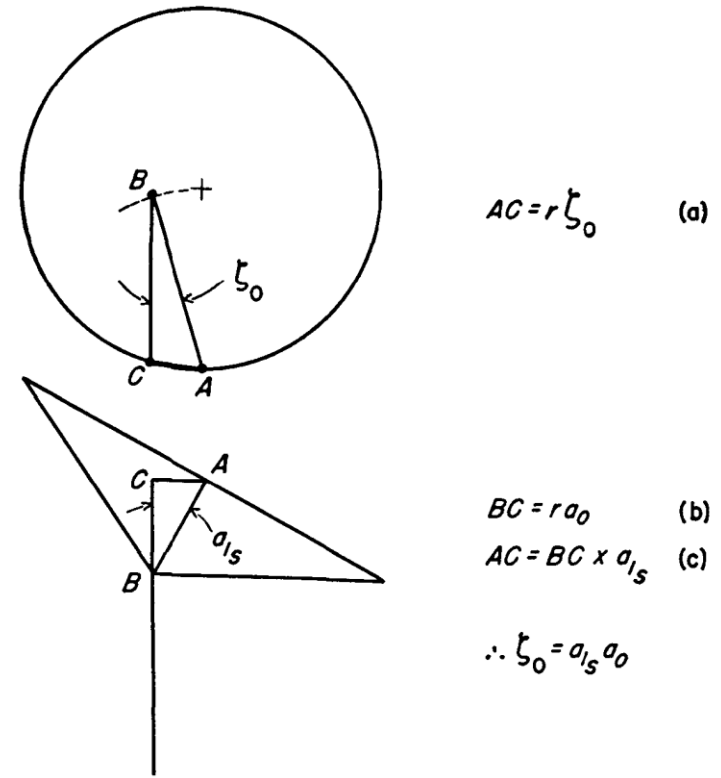


Fig. 7-39 Geometrical concept of in-plane motion.

V. Blade motion in the plane of the disk

- As the lag hinge is moved outward, the blade motion in TPP is,

$$e \neq 0 \rightarrow \zeta_{TPP} = a_0 a_{1s} \frac{\frac{3}{2} \frac{e}{R}}{\left(1 - \frac{2}{3} \frac{e}{R}\right)} \dots \omega \ll \Omega \quad (44)$$

- In Eqn. (40),

$$-I\omega^2 \zeta_0 + M \frac{R}{2} e \Omega^2 \zeta_0 = -T_b r_{a.f.} a_{1s}$$

- Setting forcing torque to 0, and solving for frequency,

$$-I\omega_n^2 = \frac{MR}{2} e \Omega^2, \omega_n = \Omega \sqrt{\frac{3}{2} \frac{e}{R}} \quad (45)$$

- Variation of blade natural frequency with lag-hinge distance ($\frac{e}{R}$) for a uniform mass blade (Fig. 7-40)

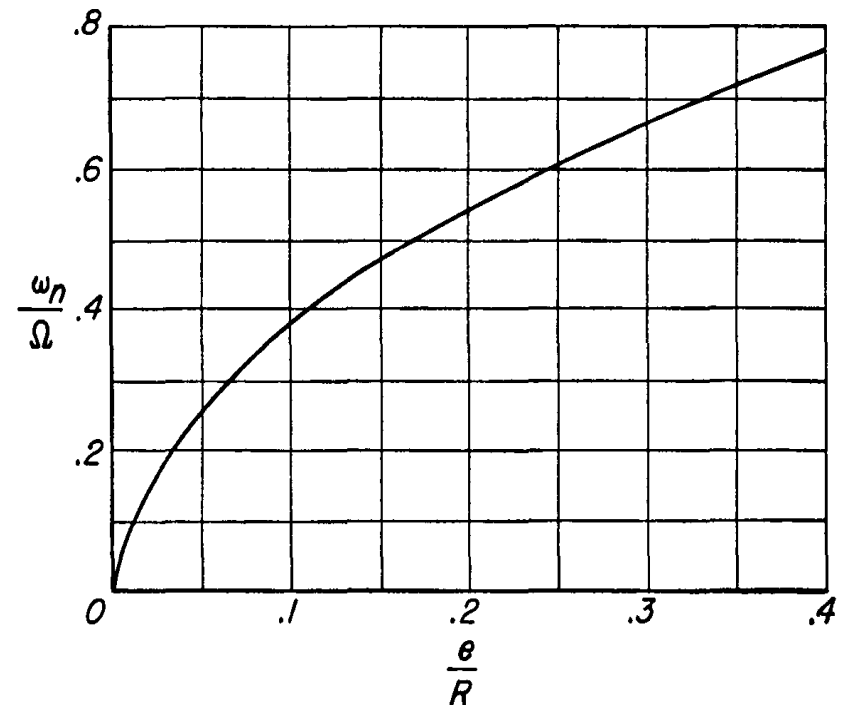


Fig. 7-40 Variation of blade natural lagging frequency with lag-hinge offset.

V. Blade motion in the plane of the disk

4. Lag motion in forward flight

- ❖ Additional exciting torque... periodic variations in blade drag
- ❖ In all practical cases, periodic in-plane blade motion is quite small $\frac{1}{2} \sim 2^\circ$
- ❖ Mean lag angle variation w.r.t. flight conditions ... much larger $10^\circ \sim (-)1^\circ$

5. Higher harmonic in-plane motion

- ❖ Although usually small compared to the first harmonics, important source of vibration (Ch. 12)
- ❖ In hover, second harmonic component exists in proportion to a_{1s}
- ❖ a_{1s} induces in-plane motion twice each revolution (Fig. 7-41)

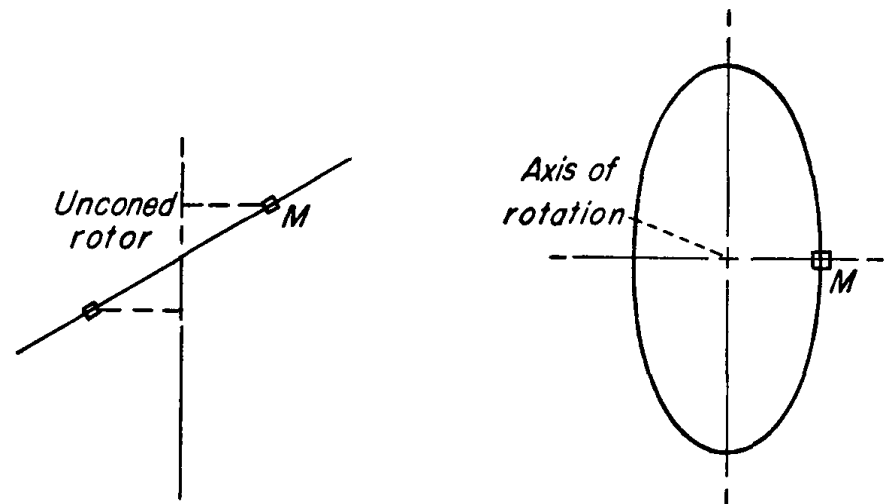


Fig. 7-41 Source of second harmonic in-plane motion in hovering.

V. Blade motion in the plane of the disk

❖ First harmonic motion $\propto a_0 a_{1s}$ (Eqn. (43))

- Eqn. (32) \rightarrow if $a_0 = 0$, only second harmonic in-plane motion exists,

$$\text{Amplitude} = \frac{1}{2} a_{1s}^2$$

- Also, second harmonic motions also arise in forward flight due to the second harmonic aerodynamic forces

❖ 4th harmonic depend on 2nd harmonic flapping

- due to Coriolis and aerodynamic
- Important for fatigue stresses and rotor vibrations
- However, small enough to be safely neglected as far as their effects on the velocities and air forces encountered by the blade are concerned